A Mathematical Model of the Modified Atmosphere Packaging (MAP) System for the Gas Transmission Rate of Fruit Produce

Li Li[1], Xi-Hong Li[1] and Zhao-Jun Ban[2]*

[1]Key Laboratory of Food Nutrition and Safety, Tianjin University of Science and Technology, Tianjin 300457, PR China

[2]Jinan Fruit Research Institute, All China Federation of Supply and Marketing Cooperatives, Shandong 250014, PR China

Summary

A mathematical model to predict oxygen, carbon dioxide, and water vapour exchanges in non-perforated and micro-perforated modified atmosphere packaging films has successfully been proposed. The transmission rate of gases was measured for films with thickness of 0.03 and 0.05 mm, perforation diameters of 0.5 and 2.0 mm, and temperatures of 0, 10 and 20 °C. Under most conditions, the increase in temperature and perforation diameter increased the transmission rate of oxygen, carbon dioxide, and water vapour, whereas the increase in film thickness decreased the transmission rate of the various gases. Validation of the proposed modified atmosphere packaging model was found to yield good prediction for gas concentrations and percentage losses in the mass of the produce after comparison with the experimental results of modified atmosphere packaging for tomato (*Lycopersicon esculentum*).

Key words: MAP, mathematical model, gas transmission rate, shelf-life of fruit

Introduction

Modified atmosphere packaging (MAP) has the potential to prolong the shelf-life of fruits or vegetables stored at cool temperatures (*1–4*). Low-permeability films limit fruit and vegetable dehydration and modify O_2 and CO_2 concentration inside the package. Low O_2 and increased CO_2 concentrations slow down respiration, which causes ripening and senescence (*4–6*). At sufficient concentrations, CO_2 may also have a fungistatic effect (*6–8*). In climacteric fruits, CO_2 inhibits ethylene synthesis and decreases the sensitivity of fruit to this gas (*9*). It can also maintain the firmness of strawberries (*8*) and induce the deterioration of fruits and vegetables, including off-flavours (*4*).

Several mathematical models describing O_2 and CO_2 exchanges in MAP have been developed, with most researchers utilizing perforations (*10–16*). However, only a few studies have developed a model that includes atmospheric gas and water vapour exchanges in MAP (*17*). Water vapour exchange in the MAP system, which affects relative humidity (RH), is considered vital because RH plays an important role in percentage losses in mass (PLM), which then influences produce quality. For instance, a high RH helps reduce rind breakdown of many varieties of citrus fruits (*18*). Meanwhile, maintaining a very high RH can encourage moisture condensation on the commodity, creating conditions favourable for microbial damage, leading to a high water loss and desiccation (*3*).

In addition, gas changes in MAP films (*i.e.* low O_2 and increased CO_2 concentrations) can affect the properties and rates of biochemical reaction *in vivo*. Ethylene synthesis indicates the ripening and deterioration of

*Corresponding author; Phone: ++86 22 6060 1425; Fax: ++86 22 6060 1341; E-mail: lili1066@yahoo.com.cn

produce in MAP films, such as bananas, tomatoes, pears, and apples (*19,20*). When O_2 and CO_2 concentrations achieve certain value, ethylene synthesis is inhibited. However, a mathematical model of ethylene concentration in MAP has rarely been estimated.

This research aims to develop a mathematical model for O_2, CO_2, ethylene, and water vapour exchanges in MAP films. To achieve this purpose, it is necessary to determine the gas transmission rate (GTR) and water vapour transmission rate (WVTR) of the MAP film, to develop a mathematical model for predicting the GTR and WVTR in the film, and to validate the proposed model when the film thickness and temperature are known.

Material and Methods

Mathematical model of the MAP system for fruit produce

MAP is important for fruit and vegetable storage and transportation. The permeability of gases and water vapour is determined as an important guideline for MAP package films. Gas molecules passing through a homogeneous membrane follow the solution-dissolution theory, which is divided into four steps: 1) adsorption, 2) solution, 3) transmission, and 4) desorption (Fig. 1).
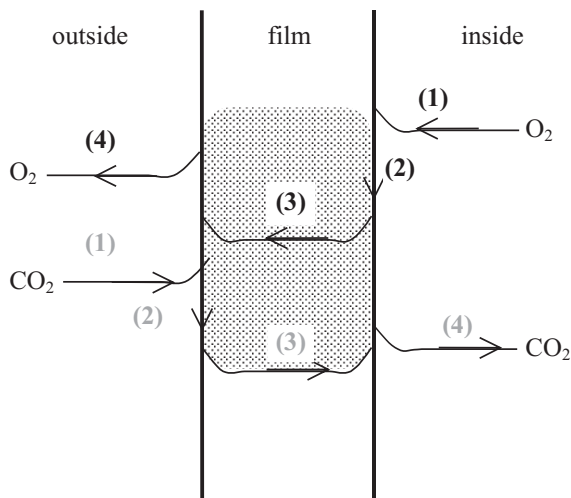

Fig. 1. Gas molecule penetrating course is divided into four steps: (1) adsorption, (2) solution, (3) transmission, and (4) desorption

The following are the key assumptions made in developing the mathematical model for MAP films: (*i*) compositions are uniformly distributed, and gas exchanges are at steady-state within the packaging; (*ii*) molecular mass transfer through the film is due to diffusion only; (*iii*) there is no adjusting component in the MAP system, and changes in gas are spontaneously modified; (*iv*) the total pressure inside the package is equal to that in the atmosphere.

Gas and water vapour exchanges through MAP films follow Fick's law as follows:

$$J_{i,film}=\frac{P_i A}{\Delta x}\left(\left[y_i\right]_a-\left[y_i\right]_p\right) \qquad /1/$$

where $J_{i,film}$ is diffusive flux of gas i per unit of time through the film (m^3/day), P_i is the gas i permeability coefficient of the film (m^3/(m·day·kPa)), A is the surface area of the film (m^2), Δx is the film thickness (m), $[y_i]_a$ is the partial pressure of gas i in the atmosphere outside the package (kPa), $[y_i]_p$ is the partial pressure of gas i inside the package (kPa), and the subscript i is substituted with O, C, E, and H to denote O_2, CO_2, ethylene, and water vapour, respectively.

In a MAP package used to store fresh produce, gas and water vapour exchanges depend on the respiration rate of the produce and the permeability of the film to gas and water vapour. The flux of gas i is a function of respiration rate, which in turn is a function of gas i concentration within the package:

$$J_{i,fruit}=m\mathrm{RR}_i\left(\left[y_i\right]_p\right) \qquad /2/$$

where $J_{i,fruit}$ is the flux of gas i per unit of time into the fruit (m^3/day), m is the mass of produce in the package (kg), and $\mathrm{RR}_i([y_i]_p)$ is the respiration rate as a function of $[y_i]_p$ (m^3/(kg·day)).

At equilibrium, the flux of gas i through the film and into the produce should be equal. Therefore, combining Eqs. 1 and 2, the following is obtained:

$$\frac{P_i A}{\Delta x}\left(\left[y_i\right]_a-\left[y_i\right]_p\right)=m\mathrm{RR}_i\left(\left[y_i\right]_p\right) \qquad /3/$$

To predict the film permeability characteristics for a sealed package containing a given mass of produce to yield a desired package gas i concentration, the following Eq. is used:

$$\frac{P_i A}{\Delta x}=\frac{m\mathrm{RR}_i\left(\left[y_i\right]_p\right)}{\left[y_i\right]_a-\left[y_i\right]_p} \qquad /4/$$

Hence, the prediction of permeability requirements should be relatively straightforward using Eq. 4 once the relationship between RR_i and the gas i concentration is known.

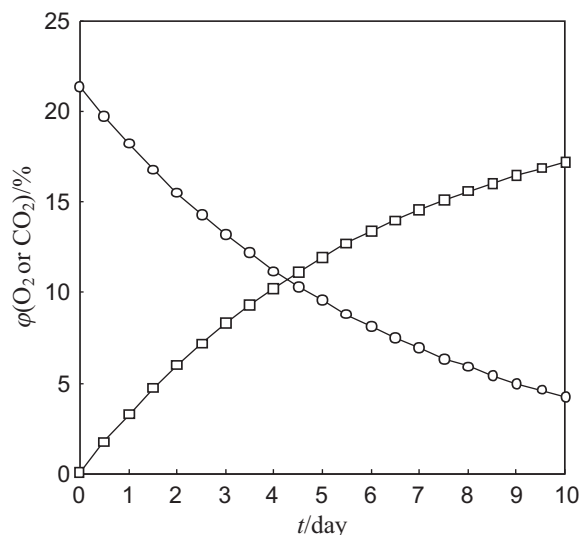An example of O_2 consumption and CO_2 production curves is shown in Fig. 2.

Fig. 2. Typical example of fitted values of predicted compositions of O_2 and CO_2 gases inside MAP film at 20 °C calculated using the mathematical model (○ O_2; □ CO_2)

The best fit equation of the data was found to have the following form:

$$[O_2] = a[1 - e^{-(b+ct)^d}]$$ /5/

$$[CO_2] = k[1 + e^{-(l+mt)^n}]$$ /6/

where $[O_2]$ is the partial pressure of O_2 in the jar (kPa), $[CO_2]$ is the partial pressure of CO_2 in the jar (kPa), t is time (day), and a, b, c, d, e, k, l, m and n are the constants of the equations.

In all cases, the R^2 values were 0.999 or better, and the fitted curves were virtually indistinguishable from the actual data (Fig. 2).

The first derivative of Eqs. 5 and 6 gives the rate of O_2 consumption and CO_2 produce *vs.* time (t) as shown below:

$$\frac{d[O_2]}{dt} = acd[(b+ct)^{d-1}]e^{-(b+ct)^d}$$ /7/

$$\frac{d[CO_2]}{dt} = -kmn[(l+mt)^{n-1}]e^{-(l+mt)^n}$$ /8/

The rate of respiration can be calculated from Eqs. 7 and 8 using the following relationship:

$$RR_{O_2} = \frac{d[O_2]}{dt} \cdot V/m$$ /9/

$$RR_{CO_2} = \frac{d[CO_2]}{dt} \cdot V/m$$ /10/

where RR_{O_2} is the O_2 consumption rate (($m^3 \cdot kPa$)/(day·kg)), RR_{CO_2} is the CO_2 production rate (($m^3 \cdot kPa$)/(day·kg)), V is the void volume of the jar (m^3), and m is the mass of the fruit in MAP bags (kg).

By combining Eqs. 7 and 9, or Eqs. 8 and 10, the relationship between time and RR_{O_2} or RR_{CO_2}, respectively, is defined as follows:

$$RR_{O_2} = acd[(b+ct)^{d-1}]e^{-(b+ct)^d}$$ /11/

$$RR_{O_2} = -kmn[(l+mt)^{n-1}]e^{-(l+mt)^n}$$ /12/

The relationship between RR_{O_2} and O_2 concentration or RR_{CO_2} and CO_2 concentration can be directly obtained by solving Eqs. 5 and 6 for time, then substituting them with Eqs. 11 and 12, respectively. This approach yields rather complex mathematical equations:

$$RR_{O_2} = cdV/m \cdot (a - [O_2])[\ln(\frac{a}{a-[O_2]})]^{\frac{d-1}{d}}$$ /13/

$$RR_{CO_2} = mnV/m \cdot (k - [CO_2])[\ln(\frac{k}{[CO_2]-k})]^{\frac{n-1}{n}}$$ /14/

An alternative approach is to simultaneously solve Eqs. 11 and 12 for time, then to generate curves that can be fitted with an approximate function.

Both Eq. 13 and Eq. 14 represent a continuous mathematical relationship between RR_{O_2} and O_2 concentration, or RR_{CO_2} and CO_2 concentration. They can be substituted with Eq. 4 to yield the equations below:

$$\frac{P_{O_2}A}{\Delta x} = \frac{cdV(a-[O_2]_p)[\ln(\frac{a}{a-[O_2]_p})]^{\frac{d-1}{d}}}{[O_2]_a - [O_2]_p}$$ /15/

$$\frac{P_{CO_2}A}{\Delta x} = \frac{mnV(k-[CO_2]_p)[\ln(\frac{k}{[CO_2]_p-k})]^{\frac{n-1}{n}}}{[CO_2]_p - [CO_2]_a}$$ /16/

Eqs. 15 and 16 can be rearranged to plot produce mass as a function of package O_2 and CO_2 concentrations, respectively, for different permeability parameters.

The advantage of MAP films is that the permeability of gas and water vapour can be adjusted to ensure that adequate gas composition and humidity conditions are achieved and maintained throughout the storage period. Moreover, the applicability of the MAP film in controlling the percentage losses in mass (PLM) of the produce inside the MAP packages has so far been rarely evaluated. The model gave a good prediction of the PLM change inside the package (Fig. 3).
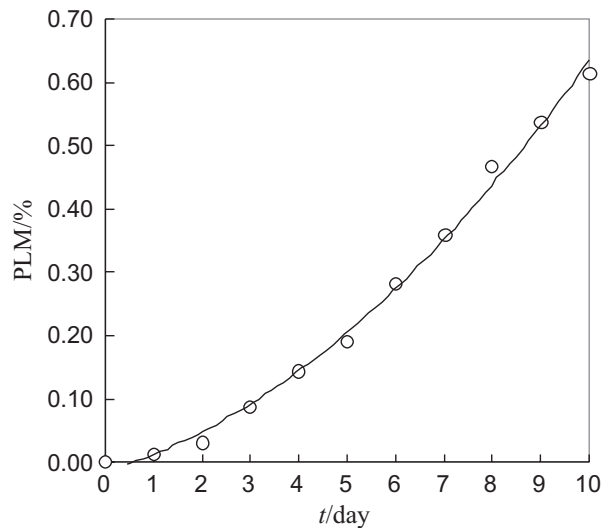

Fig. 3. Typical example of fitted values of percentage losses in mass (PLM) inside MAP film at 20 °C calculated using the mathematical model

A simplified mathematical model describing the ethylene concentration inside a package containing fresh produce is represented by Eq. 17 below:

$$[C_2H_4] = \frac{10^6 \Delta x m R_{C_2H_4}}{A P_{C_2H_4}}$$ /17/

where $[C_2H_4]$ is ethylene concentration inside the package (ppm), $R_{C_2H_4}$ is the ethylene synthesis rate of the produce (m^3/(day·kg·kPa)), and $P_{C_2H_4}$ is the permeability coefficient of the MAP film (m^3/(day·kPa)). Higher ethylene gas permeability of the film makes it less effective in attaining the optimal package atmosphere required for some slowly respiring produce.

Transmission rate through the MAP film

O_2 and CO_2

The gas transmission rate (GTR) of the MAP films of 0.03 and 0.05 mm thickness, and that of 0.05 mm thickness with 8 perforations of 0.5 and 2.0 mm diameter) for O_2 and CO_2 was determined at 0, 10 and 20 °C, respectively. The method used for determining film transmission rate followed that of Ishikawa *et al.* (*21*) with some modifications. Pure CO_2 of known volume was initially introduced into the MAP packages with 22.0×30.0 cm size. These packages were hung in a glass

jar and stored in a temperature-controlled incubator. The initial gas composition inside the jar was atmospheric. During the experiment, CO_2 permeated out of the package and into the jar, while O_2 permeated into the package. The gas concentration inside the jar was periodically measured by a gas chromatograph (GC). An example of the fit of the predicted partial pressure was observed, suggesting that the gas transmission rates were accurate. The GTR was calculated using the following:

$$\ln\left(\frac{X_{in,i,0} - X_{out,i}}{X_{in,i,t} - X_{out,i}}\right) = P_i \frac{p_T t^{\Delta x}}{V} \qquad /18/$$

where $X_{in,i,0}$ is the initial concentration of gas i inside the jar (%), $X_{in,i,t}$ is the concentration of gas i inside the jar at the time t (%), $X_{out,i}$ is the concentration of gas i outside the jar (%), P_i is the gas transmission of MAP to gas i (m³/(m·day·kPa)), Δx is the film thickness (m), p_T is the total pressure inside the package (kPa) equal to 101.325 kPa, t is time (day), and V is the void volume of the jar (m³).

Water vapour

Water vapour transmission rate (WVTR) was measured gravimetrically using the ASTM method E96-95 (22). Approximately 8 g of anhydrous calcium chloride, after drying at 60 °C for 1 h, was placed in each test jar to establish dry conditions. The relative humidity (RH) inside the jar was assumed to be 0 %. A sample of film was placed over the jar, and its edge was sealed. After the films were mounted, the whole assembly was weighed and placed in a temperature-controlled chamber at a set temperature (±1 °C) and RH of (80±2) %. Experiments were conducted at 0, 10 and 20 °C storage temperatures. Additional weighing with an accuracy of 0.001 g was done at 30-minute intervals. A similar approach was done according to Herrmann *et al.* (23) and Erdohan and Turhan (24) for measuring the water vapour permeability of methylcellulose-whey protein films. WVTR was calculated in kg/(m²·day) using:

$$\text{WVTR} = \frac{m_t - m_0}{\Delta t} \cdot \frac{1}{A} \qquad /19/$$

where m_0 is the initial mass of the test jar (kg), m_t is the mass of the test jar at time t (kg), Δt is the duration of the test period (day), and A is the effective surface area of the test film (m²).

Validation of the proposed model

To validate the mathematical model, a series of experiments was conducted. Low density polyethylene (LDPE) film package (22.0×30.0 cm) was used in all treatments. Films of 0.03 and 0.05 mm thickness, and that of 0.05 mm thickness with 8 perforations of 0.5 mm diameter were used. The gas permeability of the experimental films was determined as mentioned previously. The produce used in the MAP experiment was *Lycopersicon esculentum* (tomato), which is recognized as a high-quality late-season vegetable. Its rind is orange-red, and the flesh is red, sweet and delicious. The fruit is elliptical in shape, typically 1.0–2.5 cm in diameter and 1.5–4.0 cm in length. The optimum atmospheric composition for *Lycopersicon esculentum* is probably in the range of 3–8 % O_2 and 5–10 % CO_2. *Lycopersicon esculentum*, size

L (about 2.0 cm diameter and 3.0 cm in length), was harvested in March 2007, which is the normal commercial harvesting period, and immediately transported to our laboratory. The produce was temporarily stored at 0 °C until use in the MAP experiments.

MAP packages (500 g of *Lycopersicon esculentum*) of different thickness (0.03 and 0.05 mm) and different perforation diameters (0.5 and 2.0 mm) were studied under different temperatures (0, 10 and 20 °C). The MAP packages were sealed and then stored in a temperature-controlled incubator. The RH of the air inside the chamber was controlled by a saturated LiCl solution under 0, 10 and 20 °C. The initial gas composition was atmospheric in all trials.

Gas analysis

The gas composition inside the package was periodically analyzed. For all trials, the gas composition inside the package was measured using a gas chromatograph at 24-hour intervals for all the samples stored at three different temperatures. The method used was based on that of Ishikawa *et al.* (21) with some modifications. The measured and the predicted concentrations of the gases (O_2 and CO_2) inside the packages were then compared.

Percentage losses in mass (PLM)

The packaged samples were marked for PLM. Their initial mass was taken, and periodic observations of the loss in mass were made by weighing the samples every 24 h. PLM was calculated and expressed as cumulative percentage loss.

Consequently, the measured data were compared with those predicted using the proposed mathematical model. The goodness of fit of the model was determined by calculating the mean relative error, as reported by McLaughlin and O'Beirne (25). This method can indicate the relative error of the predictions; values below 10.0 % were considered to be reasonably good for most practical purposes.

Statistical analysis

All data were analyzed by factorial analysis or one-way analysis of variance (ANOVA). The significance of differences between means was determined by the Tukey's HSD (honestly significant difference) test at p<0.05. SPSS software for Windows v. 11.5 (SPSS Inc., IL, USA) was used for all data analyses.

Results and Discussion

Transmission rate through the MAP film

O_2 and CO_2

Temperature exerted a significant positive effect on the GTR in the tested range (Table 1). Emond *et al.* (10) reported similar results; however, Silva *et al.* (13) and Fonseca *et al.* (11) reported that temperature had no significant effect. The diffusivity of gas in air increased by about 80 % when temperature was increased from 0 to 20 °C.

Table 2 shows that there is no significant difference between the GTR when MAP films with thickness of

Table 1. Effects of temperature on permeability coefficient of MAP film to O_2 and CO_2 gases using 0.03 mm thick film

Temperature/°C	$P_i/(m^3/(10^5 \text{ m·day·kPa}))$	
	O_2	CO_2
0	(1.32±0.02)a	(1.36±0.05)a
10	(2.07±0.06)b	(2.15±0.25)b
20	(2.38±0.10)c	(2.50±0.14)c

Data are mean values of three separate experiments±standard deviation (N=7); mean values followed by different letters in each column are significantly different at p<0.05

Table 2. Effects of film thickness on permeability coefficient of MAP film to O_2 and CO_2 gases at 0 °C

Thickness/mm	$P_i/(m^3/(10^5 \text{ m·day·kPa}))$	
	O_2	CO_2
0.03	(1.32±0.02)a	(1.36±0.05)a
0.05	(1.31±0.04)a	(1.42±0.20)a
0.05 with perforations (∅=0.5 mm)	(1.77±0.01)b	(1.73±0.03)b
0.05 with perforations (∅=2.0 mm)	(3.19±0.12)c	(3.12±0.08)c

Data are mean values of three separate experiments±standard deviation (N=7); mean values followed by different letters in each column are significantly different at p<0.05

0.03 and 0.05 mm were used, whereas there was a significant increase in GTR when perforations were introduced, especially when perforation diameter was increased from 0.5 to 2.0 mm (p<0.05). Therefore, film thickness did not seem to be a dominant factor for the GTR of the non-perforated film. On the other hand, Emond *et al.* (*10*), using a plexiglass cover with thickness ranging from 1.59 to 12.7 mm, reported that an increase in film thickness decreases GTR of O_2 and CO_2. Note that the perforation diameter exerted a positive effect on GTR.

To investigate the dependence of GTR on gas type, the data obtained under the same experimental conditions (temperature and film thickness) were statistically compared (Table 3). Under most conditions, there was no significant difference in the GTR between gas types (O_2 and CO_2). The average ratio of CO_2 to O_2 permeability, the β ratio, was 1.047. This ratio did not depend on any

factor tested. Emond *et al.* (*10*), Fonseca *et al.* (*11*), and Techavises and Hikida (*26*) reported an average β ratio of 1.00, 0.81, and 1.04, respectively, which was close to the β ratio obtained here. Paul and Clarke (*12*) also reported that perforations served as a function of non-selective permeation gases. Perforations in polymeric films can change the ratio of gas transport, generally reducing the β ratio, and thereby making it possible to adjust the gas composition. In addition, the proposed model was found to fit the experimental data well, and the mean relative error between the observed and predicted values was below 8.8 %.

Water vapour

Fig. 4 summarizes the measured water vapour transmission rate (WVTR) through a series of MAP films. It is clear that the tested factors significantly affected the WVTR. Temperature showed a positive effect, whereas film thickness had a negative effect on WVTR. The WVTR values ranged from 0.27 to 1.54 $kg/(m^2 \cdot day)$, the lowest being for 0.05 mm film thickness at 0 °C, while the highest was for 0.03 mm film thickness at 20 °C. WVTR values were found to increase from 0.27 to 1.01 $kg/(m^2 \cdot day)$ and 0.45 to 1.54 $kg/(m^2 \cdot day)$ when the temperature increased from 0 to 20 °C for 0.05 and 0.03 mm film thickness, respectively. Hale *et al.* (*27*) reported that WVTR
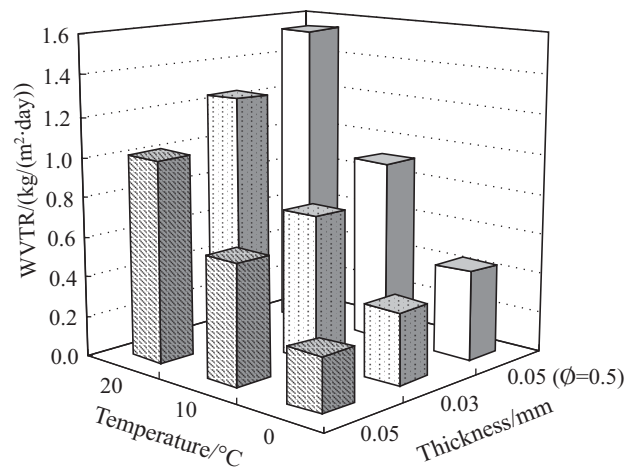
Fig. 4. Water vapour transmission rate (WVTR) ($kg/(m^2 \cdot day)$) of three series of MAP films at 0, 10, and 20 °C: 0.03 mm thick film, 0.05 mm thick film and 0.05 mm thick film with 8 perforations of 0.5-mm diameter

Table 3. Dependences of permeability coefficient on gas type under various experimental conditions using 0.03 and 0.05 mm thick films

Type of gas	$P_i/(m^3/(10^5 \text{ m·day·kPa}))$					
	Temperature/°C					
	0		10		20	
	Thickness/mm					
	0.03	0.05	0.03	0.05	0.03	0.05
O_2	(1.32±0.02)a	(1.31±0.04)a	(2.07±0.06)a	(2.04±0.01)a	(2.38±0.10)a	(2.43±0.2)a
CO_2	(1.36±0.05)a	(1.42±0.20)a	(2.15±0.25)a	(2.16±0.05)a	(2.50±0.14)a	(2.51±0.04)a

Data are mean values of three separate experiments±standard deviation (N=7); mean values followed by different letters in each column are significantly different at p<0.05

ranged from 0.97 to 4.26 kg/(m²·day) for a series of different film thicknesses and tested temperatures.

Validation of the proposed model

For the MAP storage of *Lycopersicon esculentum*, the model was found to give good prediction for the gas concentration changes inside the package at different temperatures using films with 0.03 mm thickness (Fig. 5), 0.05 mm thickness (Fig. 6) and 0.05 mm thickness with 8 perforations of 0.5 mm diameter (Fig. 7). Gas concentration was found to change faster at higher temperatures than at lower temperatures owing to the dependence of the film gas transmission rate on the temperature. Similarly, the perforation diameter exerted a positive effect. The introduction of small perforations on the film package markedly changed the package atmosphere because of the higher relative magnitude of the permeability of the perforation than the MAP film. For instance, the O_2 and CO_2 concentrations until day 5 of the produce storage in the 0.05-mm film package without perforations at 0 °C were 13.0 and 4.9 % (Fig. 6), and 19.9 and 1.1 % for the films with 0.5-mm diameter perforations (Fig. 7).

The model also gave a good prediction of the PLM change inside the package (Fig. 8). The results showed that temperature and introduction of perforations exerted a positive effect, whereas film thickness resulted in a negative effect.

All the results showed a fit between the experimental and predicted values, wherein a good agreement was established. The mean relative error between the observed and predicted values was found to be below 9.5 % for all treatments, thus confirming the predicting capability of the model. Similarly, an empirical model for predictive respiration rate was successfully developed (*28*). The mathematical model of respiration rate and the
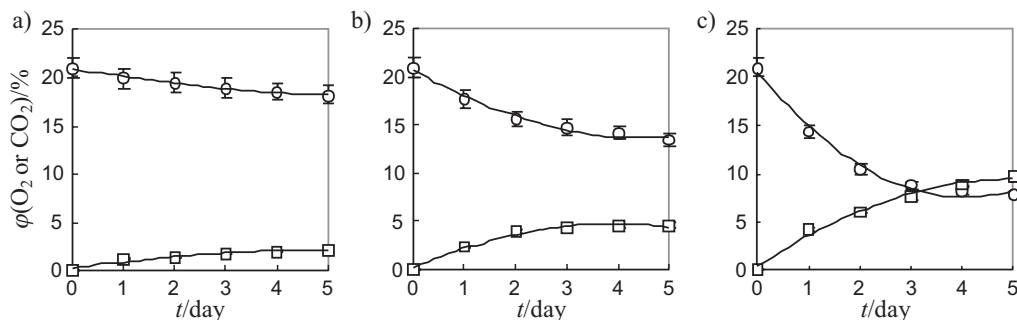

Fig. 5. Validation of the model showing the experimental and predicted gas concentrations inside MAP film packages with produce, using 0.03 mm thick film at: a) 0, b) 10 and c) 20 °C (○ O_2; □ CO_2; solid lines represent the predicted values)
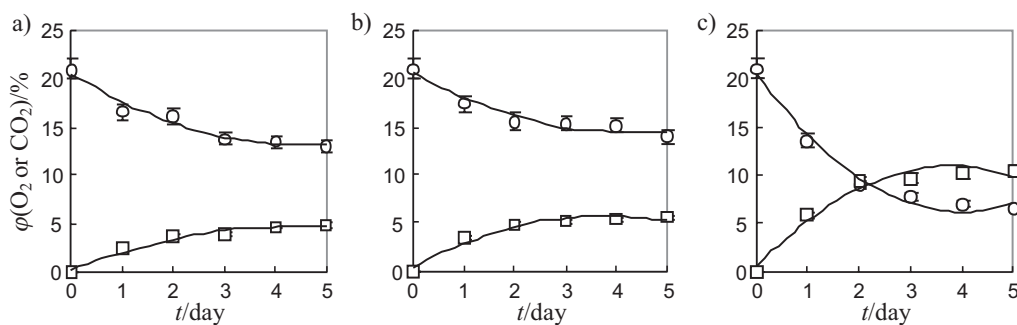

Fig. 6. Validation of the model showing the experimental and predicted gas concentrations inside MAP film packages with produce, using 0.05 mm thick film at: a) 0, b) 10 and c) 20 °C (○ O_2; □ CO_2; solid lines represent the predicted values)
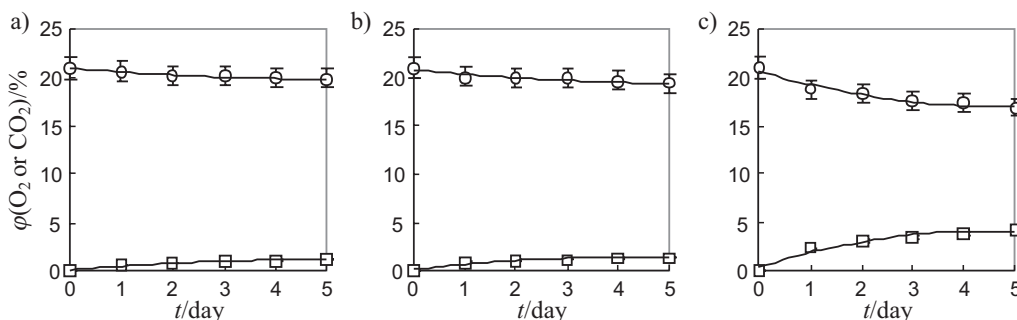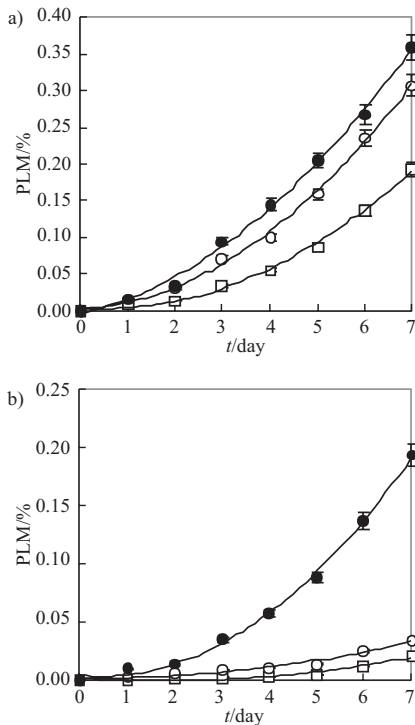

Fig. 7. Validation of the model showing the experimental and predicted gas concentrations inside MAP film packages with produce, using 0.05 mm thick film with 8 perforations of 0.5 mm diameter at: a) 0, b) 10 and c) 20 °C (○ O_2; □ CO_2; solid lines represent the predicted values)

Fig. 8. Validation of the model showing the experimental and predicted PLM of the produce inside MAP film packages, using: a) 0.03 (○), 0.05 mm (●) thick films and 0.05 mm thick film with 8 perforations of 0.5 mm diameter (□) at 20 °C, and b) 0.05 mm thick film at 0 (□), 10 (○) and 20 °C (●) (solid lines represent the predicted values)

predicted steady gas concentration of a particular kind of produce (such as tomato) in modified atmosphere packages were studied (*29–31*). The desired equilibrium gas concentration could be achieved by adjusting the data of film specification with the help of the predictive model.

Conclusions

A mathematical model with good predictions was successfully reported, which simulates changes over time in concentrations of various gases inside MAP films. The model may be used for non-perforated and micro-perforated MAP films. An increase in temperature and the introduction of perforation could increase the transmission rate of O_2, CO_2, and water vapour, whereas an increase in film thickness could decrease the transmission rate of various gases.

References

1. R.G. Tomkins, The conditions produced in film packages by fresh fruits and vegetables and the effect of these conditions on storage life, *J. Appl. Microbiol. 25* (1962) 290–307.

2. S.S. Rizvi, Requirements for foods packaged in polymeric films, *CRC Crit. Rev. Food Sci. Nutr. 14* (1981) 111–134.

3. D. Zagory, A.A. Kader, Modified atmosphere packaging of fresh produce, *Food Technol. 42* (1988) 70–77.

4. A.A. Kader, D. Zagory, E.L. Kerbel, Modified atmosphere packaging of fruits and vegetables, *CRC Crit. Rev. Food Sci. 28* (1989) 1–30.

5. G. Lopez-Briones, P. Varoquaux, G. Bureau, B. Pascat, Modified atmosphere packaging of common mushroom, *Int. J. Food Sci. Technol. 28* (1993) 57–68.

6. M.K. El-Kazzaz, N.F. Sommer, R.J. Fortlage, Effect of different atmospheres on postharvest decay and quality of fresh strawberries, *Phytopathology*, *73* (1983) 282–285.

7. T. Agar, J.M. Garcia, U. Miedke, J. Streif, Effect of high CO_2 and low O_2 concentrations on the growth of *Botrytis cinerea* at different temperatures, *Gartenbauwissenschaft*, *55* (1990) 219–222.

8. Y. Chambroy, M.H. Guinebretière, G. Jacquemin, M. Reich, L. Breuils, M. Souty, Effects of carbon dioxide on shelf-life and postharvest decay of strawberry fruit, *Sci. Aliment. 13* (1993) 409–423.

9. J.L. Cheverry, M.O. Sy, J. Pouliqueen, P. Marcellin, Regulation by CO_2 of 1-aminocyclo-propane-1-carboxylic acid conversion to ethylene in climacteric fruits, *Physiol. Plantarum*, *72* (1988) 535–540.

10. J.P. Emond, F. Castaigne, C.J. Toupin, D. Desilets, Mathematical modeling of gas exchange in modified atmosphere packaging, *Trans. Am. Soc. Agric. Eng. 34* (1991) 239–245.

11. S.C. Fonseca, F.A.R. Oliveria, I.B.M. Lino, J.K. Brecht, K.V. Chau, Modeling O_2 and CO_2 exchange for development of perforation-mediated modified atmosphere packaging, *J. Food Eng. 43* (2000) 9–15.

12. D.R. Paul, R. Clarke, Modeling of modified atmosphere packaging based on designs with a membrane and perforations, *J. Membrane Sci. 208* (2002) 269–283.

13. F.M. Silva, K.V. Chau, J.K. Brecht, S.A. Sargent, Tubes for modified atmosphere packaging of fresh fruits and vegetables: Effective permeability measurement, *Appl. Eng. Agric. 15* (1999) 313–318.

14. T. Hirata, Y. Makino, Y. Ishikawa, S. Katsuura, Y. Hasegawa, A theoretical model for designing modified atmosphere packaging with a perforation, *Trans. Am. Soc. Agric. Eng. 39* (1996) 1499–1504.

15. D.S. Lee, P. Renault, Using pinholes as tools to attain optimum modified atmospheres in packages of fresh produce, *Packag. Technol. Sci. 11* (1988) 119–130.

16. P. Renault, M. Souty, Y. Chambroy, Gas exchange in modified atmosphere packaging. 1: A new theoretical approach for microperforated packs, *Int. J. Food Sci. Technol. 29* (1994) 365–378.

17. I. Merts, D.J. Cleland, N.H. Banks, A.C. Cleland, Development of a mathematical model of modified atmosphere packaging systems for apples, *Proceedings of the 21st International Congress of Refrigeration*, Washington, DC, USA (2003).

18. R. Porat, B. Weiss, L. Cohen, A. Daus, N. Aharoni, Reduction of postharvest rind disorders in citrus fruit by modified atmosphere packaging, *Postharvest Biol. Technol. 33* (2004) 35–43.

19. S.M. Blankenship, J.M. Dole, 1-Methylcyclopropene: A review, *Postharvest Biol. Technol. 28* (2003) 1–25.

20. J.D. Mannapperuma, R.P. Singh, Micromodel optimization of modified atmosphere vegetable/fruit packaging CAP 90, *Proceedings of the Fifth International Conference on Controlled/Modified/Vacuum: Packaging-CAP 90*, San Jose, California, USA (1990).

21. Y. Ishikawa, T. Hirata, Y. Hasegawa, Development of simple gas permeability measurement for polymeric films: On high gas permeability films for MA packaging of fresh produce, *J. Packag. Sci. Japan, 6* (1997) 213–220 (in Japanese).

22. ASTM Method E96-95, Standard Test Methods for Water Vapour Transmission of Materials, American Society for Testing of Materials (ASTM) (1995).

23. P.S.P. Herrmann Jr, C.M.P. Yoshida, A.J.A. Antunes, J.A. Marcondes, Surface evaluation of whey protein films by

atomic force microscopy and water vapour permeability analysis, *Packag. Technol. Sci.* **17** (2004) 267–273.

24. Z.Ö. Erdohan, K.N. Turhan, Barrier and mechanical properties of methylcellulose-whey protein films, *Packag. Technol. Sci.* **18** (2005) 295–302.

25. C.P. McLaughlin, D. O'Beirne, Respiration rate of a dry coleslaw mix as affected by storage temperature and respiratory gas concentrations, *J. Food Sci.* **64** (1999) 116–119.

26. N. Techavises, Y. Hikida, Development of a mathematical model for simulating gas and water vapour exchanges in modified atmosphere packaging with macroscopic perforations, *J. Food Eng.* **85** (2008) 94–104.

27. W.R. Hale, K.K. Dohrer, M.R. Tant, I.D. Sand, A diffusion model for water vapour transmission through micropo-

rous polyethylene/CaCO$_3$ films, *Colloid. Surf. A*, *187–188* (2001) 483–491.

28. S.C. Fonseca, F.A.R. Oliveira, J.K. Brecht, Modelling respiration rate of fresh fruits and vegetables for modified atmosphere packages: A review, *J. Food Eng.* **52** (2002) 99–119.

29. S. Fishman, V. Rodov, S. Ben-Yehoshua, Mathematical model for perforation effect on oxygen and water vapour dynamics in modified-atmosphere packages, *J. Food Sci.* **61** (1996) 956–961.

30. S. Gong, K.A. Corey, Predicting steady-state oxygen concentrations in modified-atmosphere packages of tomatoes, *J. Am. Soc. Hortic. Sci.* **119** (1994) 546–550.

31. C.C. Yang, M.S. Chinnan, Y.C. Hung, Modeling the effect of O$_2$ and CO$_2$ on respiration and quality of stored tomatoes, *Trans. Am. Soc. Agric. Eng.* **31** (1988) 920–925.